ODOVTOS
International Journal of Dental Sciences
https://revistas.ucr.ac.cr/index.php/Odontos | ISSN: 2215-3411

BASIC RESEARCH

DOI: 10.15517/IJDS.2021.45011

Received:
9-X-2020

Accepted:
20-X-2020

Published Online:
4-XII-2020

Analysis of the Mechanical Behavior and Effect of Cyclic Fatigue on the Implant-Abutment Interface

Análisis del comportamiento mecánico y efecto de la fatiga cíclica en la interface implante-pilar

Ramón Germán Sandoval DDS, MSc[1]; Marine Ortiz Magdaleno DDS, MSc, PhD[2]; Paula Sánchez Robles DDS, MSc[1]; Norma Zavala Alonso DDS, MSc, PhD[3]; Gabriel Fernando Romo Ramírez DDS[4]

1. Specialty in Aesthetic, Cosmetic, Restorative, and Implantological Dentistry, Faculty of Stomatology, Autonomous University of San Luis Potosí, San Luis Potosí, México.
2. Specialty in Aesthetic, Cosmetic, Restorative, and Implantological Dentistry, Faculty of Stomatology, Autonomous University of San Luis Potosí, San Luis Potosí, México.
http://orcid.org/0000-0001-6033-3032
3. Department of Dental Science Advanced Education, Faculty of Stomatology, Autonomous University of San Luis Potosí, San Luis Potosí, México.
4. Specialty in Aesthetic, Cosmetic, Restorative, and Implantological Dentistry, Faculty of Stomatology, Autonomous University of San Luis Potosí, San Luis Potosí, México.
http://orcid.org/0000-0002-3945-9703

Correspondence to: Dra. Marine Ortiz Magdaleno - marine.ortiz@uaslp.mx

ABSTRACT: Purpose: The seal of the interface formed at the implant-abutment connection is essential for the long-term success of the implant-supported restoration. The aim of this study was to analyze the mechanical behavior and the effect of cyclic fatigue before and after in the marginal fit of implant-abutment according to the manufacturing technique of the abutment. Materials and methods: Machined titanium abutments (DENTIS), cast abutments with Nickel-Chromium alloy (VeraBond II), and manufacturing custom milled Zirconia abutments (Zirkonzahn) were evaluated. The implant-abutment assemblies were subjected to cyclic loads of 133 N at a frequency of 19.1 Hz for 200,000 cycles. The microgap was measured using Scanning Electronic Microscope and the distribution of compressive stress by the three-dimensional Finite Element (FE) method. Results: The microgap measurement values of the machined abutments were 1.62µm and 1.92µm, cast abutments were 14.14 µm, and 28.44 µm, and the milled abutments were 14.18µm and 20.15µm before and after cyclic fatigue, respectively. Only the cast abutments and the machined abutments showed a statistically significant difference before and after cyclic fatigue ($p \leq 0.05$). The FE analysis showed that the critical areas of compressive stress were located at the

implant-abutment connection, increasing in the cast abutments and decreasing in the milled and the machined abutments. Conclusion: Cyclic fatigue exerts an effect on the dimensions of the microgap at the implant-abutment interface before and after loading; this microgap depends of the type of abutment material and the manufacturing technique.

KEYWORDS: Abutment; Implant; Microgap; Cyclic fatigue; Compressive stress.

RESUMEN: Propósito: El sellado de la interface de la conexión implante-pilar es esencial para el éxito a largo plazo de la restauración implantosoportada. El objetivo de este estudio fue analizar el comportamiento mecánico y el efecto de la fatiga cíclica antes y después en el sellado de la conexión implante-pilar de acuerdo a la ténica de fabricación del pilar. Materiales y Métodos: Pilares mecanizados de titanio (DENTIS), pilares calcinables colados con aleación Niquel-Cromo (VeraBond II) y pilares fresados de Zirconia (Zirkonzahn) fueron evaluados. Los implantes y pilares atornillados se sometieron a una carga de 133 N a una frecuencia de 19.1 Hz durante 200 000 ciclos. El microgap fue medido con el Microscopio Electrónico de Barrido y la distribución del esfuerzo de compresión por el método tridimensional de Elemento Finito (EF). Los valores del microgap de los pilares mecanizados fueron de 1.62µm y 1.92µm, en los pilares calcinables fue de 14.14µm y 20.15µm, y los pilares fresados fue de 14.18µm y 28.44 µm antes y después de la fatiga cíclica, respectivamente. Los pilares calcinables y lo mecanizados mostraron diferencia estadísticamente significativa antes y después de la fatiga cíclica ($p \leq 0.05$). El análisis por EF mostró que las áreas críticas del esfuerzo de compresión estaban localizadas en la conexión implante-pilar, aumentando en los pilares calcinables y disminuyendo en los pilares fresados y en los mecanizados. Conclusión: La fatiga cíclica ejerce un efecto sobre las dimensiones del microgap en la interface implante-pilar antes y después de la carga cíclica; este microgap depende del tipo de material y de la técnica de fabricación del pilar.

PALABRAS CLAVE: Pilar; Implante; Microgap; Fatiga cíclica; Esfuerzo de compresión.

INTRODUCTION

An implant-supported rehabilitation includes an implant inserted into the maxillary or mandibular bone and a screw-retained prosthetic abutment. An abutment has been described as an element that serves to support and/or retain an implant-borne prosthesis, in some cases independently and in others integrated within the structure itself (1). The interface between the implant-abutment connection is the surface where the implant-abutment is connected (2,3). When there is an occlusal overload, the forces act directly on the implant-abutment connection and on the interface of the implant-bone tissue causing a loss of osseointegration (4).

The selection of the prosthetic abutment depends on several factors, such as the depth of the implant in relation to the thickness of the gingival tissue, the aesthetic needs, the correction of the parallelism of the implants, and the space available for the restoration. According to the material used, there are abutments of Titanium, Cobalt-Chrome (Cr-Co) and Nickel-Chrome (Ni-Cr) alloys, and ceramic abutments

made of Alumina Oxide and Zirconium Oxide that significantly improve the aesthetic result. According to their type of manufacture, these are classified as prefabricated, cast abutments known as Universal Clearance Limited Abutment (UCLA), which are cast in metal alloys, and custom milled abutments with Computer-Aided Design/Computer Assisted Manufacture (CAD-CAM) technology (5-6). The correct election of design, manufacture, and abutment material are factors that relate to soft tissue remodeling and integration and of course, to treatment success (7).

The lack of the sealing of the implant-abutment interface gives rise to mechanical and biological problems, the accumulation of bacteria that induce inflammatory tissue infiltration known as peri-implantitis, which in turn generates a loss of crestal bone, and the mechanical complications of a poor fit causes the loss of implant stability (8). This marginal misfitting has been related to a key factor in load transmission to the peri-implant bone, in that it prevents passive fit between the implant-prosthetic, which causes the loosening and fracture of the screw and even the restoration itself (9).

The mechanical behavior and transmission of forces from the abutment to the implant depends on the material of the abutment, each material possesses different mechanical properties. Prior simulation of the masticatory loads on the abutments indicates the areas where the highest concentration of stress is undergone; material fatigue is the phenomenon whereby the behavior of materials varies when they are subjected to cyclic fatigue and when the acting loads are static (10). The testing of cyclic fatigue has been considered a reliable method of generating data on the efficiency and longevity of implant-abutments, analyzing whether micro-movements cause the loosening of screws and determine the biomechanical behavior of the connection's abutment-implant (11). Another test widely used in implantology is the 3D Finite Element (FE) method, which evaluates the stress distribution in implants and the transmission of forces in the peri-implantary bone (12).

For an implant-supported restoration to be successful in the long term, the quality of the implant-abutment interface is one of the main factors for the maintenance of bone and soft tissue (13). A perfect seal in terms of mechanical precision between the implant-abutment does not imply that this is not an obstacle for the free passage of microorganisms (14-16). The aim of this study was to evaluate the effect before and after cyclic fatigue on microgap formation at the implant-abutment connection. The horizontal microgap formed between the implant and different types of abutments was measured and compared with Scanning Electron Microscopy (SEM). 3D modeling and simulation of the mechanical behavior was performed to evaluate the distribution of the compressive stress by FE analysis.

MATERIALS AND METHODS

SAMPLE PREPARATION

Thirty internal hexagonal connection implants (4.5 x 5.5mm; DENTIS) were place with a parallelometer in molds in autopolymerizing acrylic resin (Technovit 4000; Kulzer GmbH, Wehrheim, Germany) with a Young modulus of 12 GPa to simulate the elastic reaction of cortical bone during the fatigue assay, as specified in International Organization for Standardization (ISO) 14801:2016.24 (17). The 30 implants were randomly divided into three groups (n=10). The anti-rotational abutments evaluated were: machined titanium abutments (DENTIS; CA, USA); cast abutments with Ni-Cr alloy (VeraBond II; Aalba Dent, Ca, USA), and manufacturing custom milled Zirconia abutments (Zirkonzahn, USA).

The machined abutments were obtained directly from the manufacturer (DENTIS), with a

length of 5.5mm and a diameter of 2mm, and the abutment screw with a length of 6mm was used. The cast abutments were waxed to the same basic shape as machined abutments. After waxing and shaping, the internal hexagonal abutment recesses was carefully cleaned with alcohol and were individually invested with phosphate-bonded investment (GC Fuji; Tokyo, Japan) and cast with the Ni-Cr alloy (VeraBond II; AALBA Dent) following the manufacturer's instructions using the conventional lost-wax casting technique. Castings were allowed to bench-cool and were then divested and cleaned. This was followed by airborne particle abrasion with aluminum oxide granulation of 100µm under a pressure of 5 kg/cm², protecting the abutment-implant interface. No further polishing and finishing were performed. The manufacturing custom milled Zirconia abutments were fabricated using an inEOS scanner, with INlab ED software and a milling machine (Zirkonzahn) with the same shape as machined abutment.

The implant fixture and abutment were tightened to a torque of 30 Ncm utilizing a digital torque gauge. The cyclic-loading test to mimic mastication was performed on a Material Testing System cyclic loading machine with an axial load of 133 N, at a distance of 1mm from the center of the abutment, at a frequency of 19.1 Hz for 200,000 cycles. The load was applied in the direction of the longitudinal axis of the implant/abutment assembly. The tests were performed at room temperature.

MICROGAP MEASUREMENT WITH SEM

Four specific points were marked on each side of the implant to measure the horizontal gap, the microgap was measured as the minimal distance from one point of the fixture's edge to a line determined by the least squares of points at the abutment edge. Three measurements were recorded and a mean value was obtained for each side. The final horizontal misfit of each abutment was obtained as a mean of all four sides and was measured before and after cyclic loading. The samples were covered with gold nanoparticles, placed in the SEM (JSM-6510; JEOL, Tokio, Japan) at an inclination of 45º, and observed under 30X and 1000X magnification.

SIMULATION OF MECHANICAL BEHAVIOR

The measured and scanned data were transferred to the modeling software (Auto CAD2010, Solid Works 2012) to provide solid models (Figure 1). After the virtual reconstruction, the models were exported for editing the models and the configuration in relation to the mechanical properties according to their Young modulus and the Poisson ratio, in agreement with the literature (18-20) (Table 1) a force of 300 N was applied to the central node on the top surface of the abutments to simulate the occlusal loads (21). 3D FE analysis was employed to estimate stress distribution in structures subjected to mechanical loading. The implant, screw, and MTA were made of a Titanium-Aluminum-Vanadium alloy (Ti-6Al-4V), according to ISO 5832-3.29 (22). The parameters of maximal equivalent stress, maximal shear stress, unit deformation, and minimal safety factor were determined.

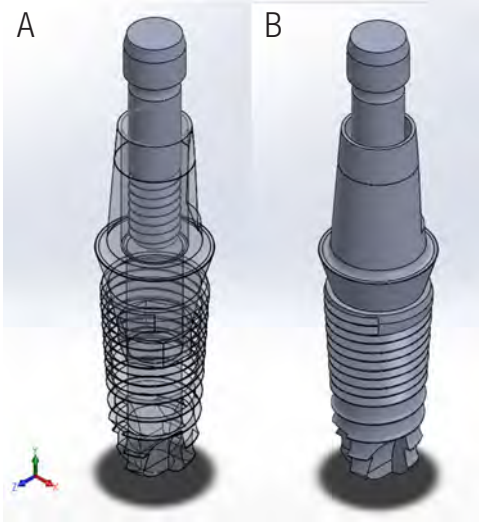

Figure 1. Simulation of the implant (A), prosthetic attachment, and fixation screw in the Solid Works program (B).

Table 1. Mechanical properties of the prosthetic abutments and implants used in FE analyses.

Abutment-Material	Young modulus (GPa)	Poisson ratio
Machined titanium and implant analogue and screw (Ti-6AL-4V)	115	0.35
Cast (Nicke-Chromium, VeraBond II)	82	0.25
Milled Zirconia	200	0.3

STATISTICAL ANALYSIS

Data were analyzed using Prism 7 for Mac OS X version 7.0 statistical software (GraphPad Software, Inc.), means and Standard Deviations (SD) were calculated for the gap variable in all study groups. One-Way ANOVA and T test statistical analyses were utilized to search for statistically significant differences in the means of the study variable among the study groups; a significance level of $p \leq 0.05$ was used.

RESULTS

Microgap mean values before the cyclic fatigue test were lower in machined abutments with 1.62±0.52µm (Figure 2. A and B), cast abutments were 14.14±1.35 µm (Figure 2. C and D), and milled abutments obtained the highest values of implant-abutment discrepancy with 14.18±6.61µm (Figure 2. E and F). Machined abutments exhibited a statistically significant difference with the cast abutments and milled abutments ($p \leq 0.05$). The results of microgap values before the cyclic fatigue test are presented in Table 2. After the cyclic fatigue test, microgap values in machined, cast and milled abutments increased compared with the cyclic fatigue data before the assay. The lowest values were obtained for machined abutments with 1.92±1.26µm (Figure 3. A and B), milled abutments continued with 20.15±4.07µm (Figure 3. C and D), and cast abutments obtained the highest microgap increases with 28.44±5.84µm (Figure 3. E and F). Statistically, there was a significant difference in the comparison among the three evaluated abutments ($p \leq 0.05$). Cast and milled abutments demonstrated a statistically significant difference ($p \leq 0.05$) before and after the cyclic fatigue test (Table 2).

SIMULATION OF THE MECHANICAL BEHAVIOR OF ABUTMENTS

The results obtained in the simulation of the behavior of the abutment and the implant system are depicted in Table 3. Milled abutments required a higher equivalent effort and their minimal safety factor was the highest compared to cast and machines. The milled abutments obtained the lowest value of unitary deformation, indicating that they required more effort for their deformation; however, MTA obtained the highest short effort compared to cast and milled abutments.

Figure 4 presents the equivalent stress analysis of the compressive stress distribution of machined (Figure 4. A), cast (Figure 4. B), and milled abutments (Figure 4. C). Warm colors indicate the highest values, therefore the critical regions in the evaluate abutments, as well as the areas where the highest percentage of deformation and highest stress concentration. In machines, cast, and milled abutments, the critical areas were located at the height of the coupling with the occlusal screw and at the top of the abutments where the load was received. A higher concentration of stress and compressive stress was observed in milled and cast abutments, and in the case of machined abutments were lower.

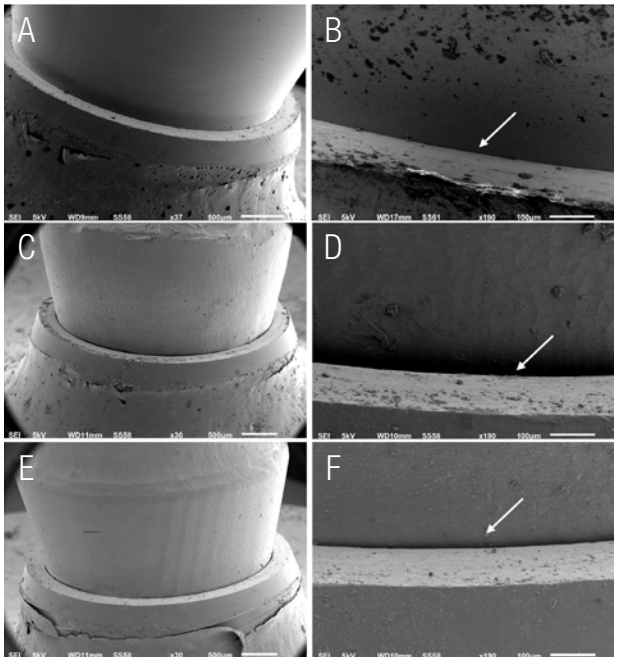

Figure 2. Micrographs of implant-abutment microgap discrepancy shown under SEM before cyclic loading. Macroscopic images were taken at 30X and at higher magnification at 1000X, with machined (A,B), cast (C,D), and milled (E,F). The arrows indicate the dimensions of the microgap.

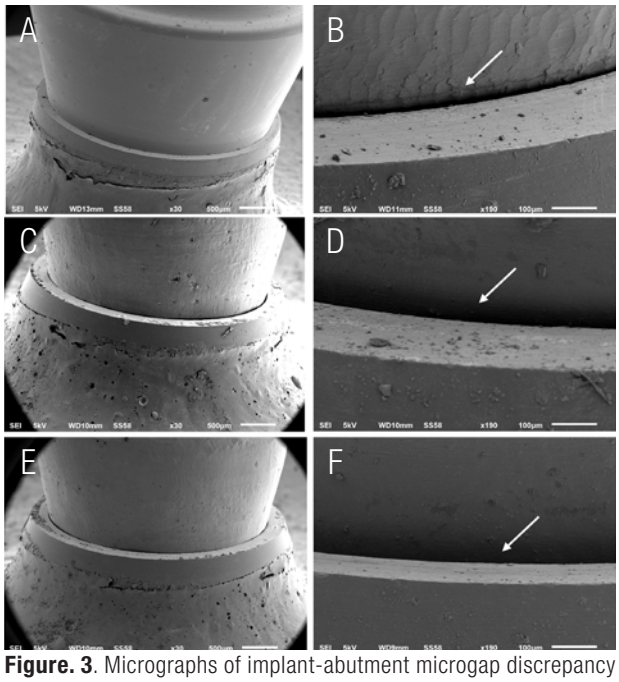

Figure. 3. Micrographs of implant-abutment microgap discrepancy shown under SEM after cyclic loading. Macroscopic images were taken at 30X and at a higher magnification at 1000X, with machined (A,B), cast (C,D), and milled (E,F). The arrows indicate the dimensions of the microgap.

Table 2. Abutment gap discrepancy before and after the cyclic fatigue test. Means followed by the same lower-case letter within any column are not statistically different and the means followed by upper case letters are statically different. *Significant difference before and after cyclic loading.

Mean Values and Standard Deviations for horizontal misfit (µm)		
Experimental group	**Before cyclic fatigue**	**After cyclic fatigue**
Machined	1.62 ± 0.52^{A}	1.92 ± 1.26^{a}
Cast	14.14 ± 1.35^{BA}	$28.44 \pm 4.07^{ba*}$
Milled	14.18 ± 6.61^{cA}	$20.15 \pm 5.84^{cab*}$

Table 3. Results of the stress-distribution simulation of abutment models.

Experimental group	Maximal equivalent effort (MPa)	Maximal short effort (MPa)	Unit deformation (mm/mm)	Minimal safety factor
Machined	570.12	404.31	4.82E-03	1.45
Cast	582.09	383.81	6.07E-03	1.51
Milled	589.24	385.77	0.0058068	1.53

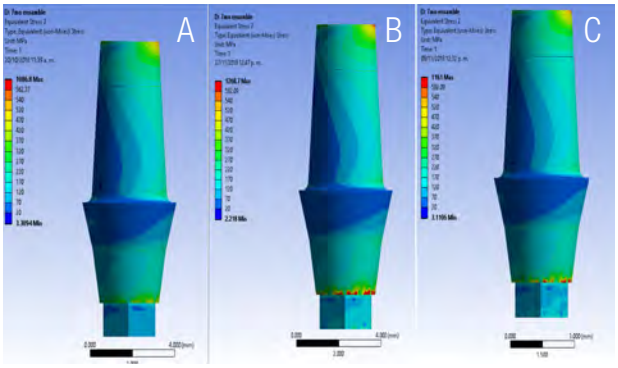

Figure 4. Results of the analysis of the distribution of compressive stress on machined (A), cast (B), and milled (C). Maximal tensions (red color) were located at the implant-abutment connection.

DISCUSSION

An interface must exist between the mechanical implant-abutment connection to ensure a seal between the two-surface connection and achieve a transitional fit (23). All implants have an interface between the implant-abutment at initial torque and prior to masticatory loading, regardless of the type of connection (24). The objective of this study was to evaluate the effect of cyclic fatigue on the formation of a microgap before and after loading. Three commonly used abutment types were evaluated: machined, cast, and milled abutments. The observation technique used to detect the microgap was SEM in the present study. The results obtained in this study demonstrated the formation of a microgap before and after cyclic fatigue; the dimensions of a microgap increased in all of the abutments evaluated after the cyclic fatigue test. Statistically, the cast and milled abutments groups revealed significant differences in microgap values before and after loading, except for machined abutments. Thus, we can induce that cyclic fatigue does have an effect on microgap formation and dimensions in the cast and milled abutments; however, apparently this effect will depend on the manufacturing material of the abutment; as the study by Sen *et al*. (25) reported that the sealing and marginal fit of abutments were affected by the type of abutment material and connection design.

Our results are in agreement with Blum *et al*. (26) who reported that a microgap in the implant-abutment interface exist before cyclic fatigue and also increases after the load. De Jesus Tavarez *et al*. (27) is in agreement with our results, reporting that mismatch values of the implant-abutment interface increased after cyclic loading in groups that presented high misfit values before loading.

In our study, we showed that the dimensions of the microgap prior to cyclic fatigue were lower than the values obtained after applying the load. Therefore, the cyclic fatigue test induces an increase of the implant-abutment microgap. Studies have reported that cyclic fatigue tests induce micro-movements that could microscopically wear away rough areas of the connected implant-abutment surfaces, contributing to screw loosening and giving rise to vertical and horizontal misfit (28). However, another factor on which the formation of a microgap depends is the decision on material type, abutment fabrication, and connection design (29).

In this study, machined abutments obtained the lowest values of microgap dimensions, showing no statistically significant difference before and after cyclic fatigue. Tsuge *et al*. (30) reported microgap values in machined abutments between 2.3µm and 5.6µm for internal connection implants. In our study, machined abutments obtained lower values of between 1.62µm and 1.92µm before and after cyclic fatigue, respectively without showing any significant difference. A possible explanation for the presence of a machined abutments misfit is by impressions during fabrication of the elements (31).

On the other hand, cast abutments in our results obtained microgap dimensions with values of 14.14µm and 20.15µm before and after cyclic fatigue. De Jesus Tavarez *et al*. (27) reported that cyclic fatigue is a factor that has been shown to increase the mismatch of cast abutments in implants with external hexagon and internal

octagonal connection. Our results are in agreement with Byrne *et al*. (32) who compared cast vs. machined fit, the machined abutments showing less microgap (15µm-35µm) than of cast abutments (66µm-68µm). In this study, cast abutments and milled abutments showed higher magnitudes of microgap than machined abutments. These gaps of the cast abutments were probably associated with limitations in casting technique, temperature-induced changes and finishing procedures (32).

Under some clinical situations, the use of ceramic abutments is a requirement for patients with aesthetic gingival biotype, milled abutments have shown excellent aesthetic effects and biomechanical properties (33). Sui *et al*. (22) reported a microgap of 19.38µm in milled abutments in internal hexagon implants, suggesting that the size of the microgap may affect the fracture resistance of the abutments. In our study, we obtained values of 14.18µm and 20.15µm before and after the cyclic fatigue test, respectively. Milled abutments may benefit from improved machining tolerance, which would result in an interface microgap comparable to that observed at the interface of a milled abutments-implant. Current results suggest that a large microgap or poor seating of the milled abutment, along with its high Young modulus, may result in deformation of the body of the implant (33). Sen *et al*. (34) published that abutment material and connection design affect the fatigue survival of the implant-abutment assembly and that milled abutments have less resistance to failure than machined abutments, its results reported marginal misfit values in the range of 2.7-4.0µm for machined abutments and 1.8-5.3µm for machined abutments. Baixe *et al*. (35) reported the size of the microgap in the range of 0.25 to 18.93µm for milled abutments with tri-channel connection.

Furthermore, milled abutments have been reported to be sensitive to functional loading and prone to fracture, especially at the connection of the abutment to the implant body; its strong, hard, and more abrasive material characteristics may affect the mechanical reliability of implant-abutment connections. The Young modulus of Zirconia is higher than that of titanium; thus, the tolerance of milled abutments in titanium implants is lower than that of machined abutments in titanium implants (36,37). The increased of the microgap for milled abutments compared to machined abutments has been reported as possibly due to the lower recommended torque values used to tighten the milled abutments (38). In this study the same torque value of 30 Ncm was used for the abutments evaluated following the manufacturer's instructions.

With regard to the simulation of mechanical behavior with FE, the three abutments demonstrated similar behavior. Distribution of the compressive stresses is located on the three abutments in the area of the implant-abutment connection where the screw head is found. Cast and milled abutments obtained higher critical zones of compressive stress than machined abutments. Our results are in agreement with Sannino *et al*. (38) who reported that the maximal stresses were located at the emergence profile of the abutment, Cho *et al*. (39) demonstrated a high stress concentration at the lower contact area of the implant-abutment interface. Also evaluated two abutment types hexagonal and conical, obtained that the abutments showed similar stress distributions (40).

Differences in the materials of the abutment-implant complex can compromise the initial integrity of the interface and can further weaken under cyclic fatigue conditions. The evaluation of the sealing ability of different materials in abutments is of primary importance in clinical practice. A limitation of this study relates to the number of implants included in each group. However, clinical studies are needed to determine the significance of discrepancies caused by lack-of-fit at the abutment-implant interface. Further *in vitro* and *in vivo* studies are necessary to determine the

effect of the cyclic fatigue on the marginal fitting of implant-abutment.

CONCLUSION

Within the limitations of the reported *in vitro* studies, cyclic fatigue is a determining factor in the dimensions of the microgap in machined, cast, and milled abutments before and after loading. The three types of abutments evaluated prior to receiving cyclic fatigue already presented a microgap with lower values in behavior than the results obtained after cyclic fatigue. Therefore, the formation of this microgap depends on the type of abutment material and manufacture. After the cyclic fatigue test, microgap values increased in machined, cast, and milled abutments; only cast and milled abutments exhibited a significant difference before and after the cyclic fatigue test. Simulation of the distribution of compressive stress revealed that the most critical areas of maximal stress are at the implant-abutment interface, increasing at cast and milled abutments.

CONFLICT OF INTEREST

The authors of the present study declare that they have nor conflict of interest.

ETHICAL APPROVAL

This article does not contain any studies with human participants or animals performed by any of the authors.

ACKNOWLEDGEMENTS

This work was supported by a grant to Ramón Francisco Germán Sandoval as a CONACYT fellow (Grant 816194/618548).

REFERENCES

1. Broggini N., McManus LM., Hermann JS., Medina RU., Oates TW., Schenk RK., et al. Persistent acute inflammation at the implant-abutment interface. J Dent Res. 2003; 82 (3): 232-237.
2. Asvanund P., Morgano M. Photoelastic stress analysis of external versus internal implant-abutment connections. J Prosthet Dent. 2011; 106 (4): 266-271.
3. Gil F.J., Herrero-Climent M., Lázaro P., Ríos JV. Implant-abutment connections: influence of the de- sign on the microgap and their fatigue and fracture behavior of dental implants. J Mater Sci: Mater Med. 2014; 25 (7): 1825-1830.
4. Bacchi A., Consani RLX., Mesquita MF., dos Santos MBF. Stress distribution in fixed-partial prosthesis and periimplant bone tissue with different framework materials and vertical misfit levels: a three-dimensional finite element analysis. J Oral Science. 2013; 55 (3): 239-245.
5. Hu M., Chen J., Pei X., Han J., Wang J. Network meta-analysis of survival rate and complications in implant-supported single crowns with different abutment materials. J Dent. 2019; 88: 103115.
6. Dantas T.S., Silveira Rodrigues R.C., Naves L.Z., Lapria Faria A.C., Palma-Dibb R.G., Ribeiro R.F. Effects of surface treatments on mechanical behavior of sintered and pre-sintered yttria-stabilized zirconia and reliability of crowns and abutments processed by CAD/CAM. Int J Oral Maxillofac Implants. 2019; 34 (4): 907-919.
7. Welander M., Abrahamsson I., Berglundh T. The mucosal barrier at implant abutments of different materials. Clin Oral Implants Res. 2008; 19 (7): 635-641.

8. Abrahamsson I., Berglundh T., Lindhe J. The mucosal barrier following abutment dis/reconnection. An experimental study in dogs. J Clinical Periodontol. 1997; 24 (8): 568-572.
9. Larrucea Verdugo C., Jaramillo Núñez G., Acevedo Avila A., Larrucea San Martín C. Microleakage of the prosthetic abutment/implant interface with internal and external connection: in vitro study. Clin Oral Implants Res. 2014; 25 (9): 1078-1083.
10. Rack A., Rack T., Stiller M., Riesemeier H., Zabler S., Nelson K. In vitro synchrotron-based radiography of micro-gapformation at the implant-abutment interface of two-piecedental implants. J Synchrotron Rad. 2010; 17 (2): 289-294.
11. Zabler S., Rack T., Rack A., Nelson K. Fatigue induced deformation of taper connections in dental titanium implants. Int. J Mater Res. 2012; 103 (2); 207-216.
12. Baggi L., Cappelloni I., Di Girolamo IM., Maceri F., Vairo G. The influence of implant diameter and length on stress distribution of osseointegrated implants related to crestal bone geometry: A three-dimensional finite finite element analysis. J Prosthet Dent. 2008; 100 (6): 422-431.
13. Jansen V., Conrads G., Richter E. Microbial leakage and marginal fit of the implant-abutment interface. Int J Oral Maxillofac Implants. 1997; 12 (4): 527-540
14. Quirynen M., van Steenberghe D. Bacterial colonization of the internal part of two-stage implants. An in vivo study. Clin Oral Impl Res. 1993; 4 (3): 158-161.
15. Keller W., Brägger U., Mombelli A. Peri-implant microflora of implants with cemented and screw retained suprastructures. Clin Oral Impl Res. 1998; 9 (4): 209-217.
16. Gross M., Abramovich I., Weiss EI. Microleakage at the abutment-implant interface of osseointegrated implants: a comparative study. Int J Oral Maxillofac Implants. 1999; 14 (1): 94-100.
17. International Organization for Standardization. ISO 14801:2016. Dentistry–implants-dynamic fatigue test for endosseous dental implants. Geneva: International Organization for Standardization; 2016. Available at: http://www.iso.org/iso/home.html
18. Çağlar A., Turhan Bal B., Karakoca S., Aydın C., Yılmaz H., Sarısoy Ş. Three-dimensional finite element analysis of titanium and yttrium-stabilized zirconium dioxide abutments and implants. Int J of Oral & Maxillofac Implants. 2011; 26 (5): 961-969.
19. Ozen J., Caglar A., Beydemir B., Aydin C., Dalkiz M. Three-dimensional finite element stress analysis of different core materials in maxillary implant-supported fixed partial dentures. Quintessence Int. 2007; 38 (6): 355-363.
20. Bidez MW., Misch CE. Force transfer in implant dentistry: basic concepts and principles. J Oral Implantol. 1992; 18 (3): 264-274.
21. Barry M., Kennedy D., Keating K., Schauperl Z. Design of dynamic test equipment for the testing of dental implants. Materials and Design. 2005; 26 (3): 209-216.
22. ISO 5832-3:1996 (E). Implants for Surgery-Metallic Materials-Part 3: Wrought Titanium 6-Aluminium 4 Vanadium Alloy. Geneva:International Organization for Standatrization 1996;42.
23. Sui X., Wei H., Wang D., Han Y., Deng J., Wang Y., et al. Experimental research on the relationship between fit accuracy and fracture resistance of zirconia abutments. J Dent. 2014; 42 (10): 1353-1359.
24. Binon PP., McHugh MJ. The effect of eliminating implant/abutment rotational misfit on screw joint stability. Int J Prosthodont. 1996; 9 (6): 511-519.
25. Şen N., Şermet IB., Gürler N. Sealing capability and marginal fit of titanium versus zirconia abutments with different connection designs. J Adv Prosthodont. 2019; 11 (2): 105-111.

26. Blum K., Wiest W., Fella C., Balles A., Dittmann J., Rack A., et al. Fatigue induced changes in conical implant-abutment connections. Dent Mater. 2015; 31 (11): 1415-1426.
27. Jesus Tavarez RR., Bonachela WC., Xible AA. Effect of cyclic load on vertical misfit of prefabricated and cast implant single abutment. J Appl Oral Sci. 2011; 19 (1): 16-21.
28. Faot F., Suzuki D., Senna PM., da Silva WJ., de Mattias Sartori IA. Discrepancies in marginal and internal fits for different metal and alumina infrastructures cemented on implant abutments. Eur J Oral Sci. 2015; 123 (3): 215-219.
29. Dibart S., Warbington M., Su MF., Skobe Z. In vitro evaluation of the implant- abutment bacterial seal: the locking taper system. Int J Oral Maxillofac Implants. 2005; 20 (5): 732-737.
30. Tsuge T., Hagiwara Y., Matsumura H. Marginal fit and microgaps of implant-abutment interface with internal anti-rotation configuration. Dent Mater J. 2008; 27 (1): 29-34.
31. Khraisat A., Abu-Hammad O., Al-Kayed AM., Dar-Odeh N. Stability of the implant/abutment joint in a single tooth externalhexagon implant-system: clinical and mechanical review. Clin Implant Dent Relat Res. 2004; 6 (4): 222-229
32. Byrne D., Houston F., Cleary R., Claffey N. The fit of cast and premachined implant abutments. J Prosthet Dent. 1998; 80 (2): 184-192.
33. Cavusoglu Y., Akça K., Gürbüz R., Cehreli MC. A pilot study of joint stability at the zirconium or titanium abutment/titanium implant interface. Int J Oral Maxillofac Implants. 2014; 29 (2): 338-343.
34. Sen N., Us YO. Fatigue survival and failure resistance of titanium versus zirconia implant abutments with various connection designs. J Prosthet Dent 2019; 122 (3): 315.e1-315.e7.
35. Baixe S., Fauxpoint G., Arntz Y., Etienne O. Microgap between zirconia abutments and titanium implants. Int J Oral Maxillofac Implants. 2010; 25 (3): 455-460.
36. Klotz MW., Taylor TD., Goldberg AJ. Wear at the titanium-zirconia implant-abutment interface: a pilot study. Int J Oral Maxillofac Implants. 2011; 26 (5): 970-975.
37. Naveau A., Rignon-Bret C., Wulfman C. Zirconia abutments in the anterior region: A systematic review of mechanical and esthetic outcomes. J Prosthet Dent. 2019; 121 (5): 775-781.e1.
38. Sannino G., Barlattani A. Mechanical evaluation of an implant-abutment self-locking taper connection: finite element analysis and experimental tests. Int J Oral Maxillofac Implants. 2013; 28: 17-26.
39. Cho SY., Huh YH., Park CJ., Cho LR. Three-Dimensional Finite Element Analysis on Stress Distribution of Internal Implant-Abutment Engagement Features. Int J Oral Maxillofac Implants. 2018; 33 (2): 319-327.
40. Cho SY., Huh YH., Park CJ., Cho LR. Three-dimensional finite element analysis of the stress distribution at the Iinternal implant-abutment connection. Int J Periodontics Restorative Dent. 2016; 36: 49-58.